2
Synthesis and Characterization Techniques of MoS_2

2.1 SYNTHESIS OF MoS_2

In the last decade, for the synthesis of MoS_2 on different substrates, various techniques have been developed. Among different techniques, mechanical exfoliation, liquid exfoliation, chemical vapor deposition, and hydrothermal synthesis are most commonly used. Some of the methods offer batter control over various parameters of the deposited film as compared to the other methods. In this section, we briefly explain some of the techniques which have been used in this thesis work.

2.1.1 Mechanical exfoliation

Mechanical exfoliation is the most widely used method for the deposition of the monolayer to few-layer 2D materials on various substrates. Since the isolation of graphene from a graphite crystal through mechanical exfoliation in 2004, this method still maintains its popularity due to its meager cost, high-quality flakes, and simple deposition mechanism(Yi and Shen, 2015). Most of the properties of nearly all the newly discovered 2D layered materials have been studied on exfoliated flakes(Chen et al., 2015).

The mechanical exfoliation process of MoS2 is illustrated in Figure 2.1. In this method, we use a commercially available crystal of molybdenite (SPI Supplies) and scotch-tape. Firstly, some layers got transferred from crystal to scotch tape. Then we do repeat peeling to achieve monolayer to few-layer MoS2 flakes. And finally, the flakes got transferred from scotch tape to the substrate. The typical flake size is of the order of micrometers by using this technique. Three different mechanically exfoliated flakes of different sizes deposited over a SiO_2/Si substrate are shown in Figure 2.2. These flakes are contacted using the 0.6 µm resolution lens.

This method remains the first choice of researchers to understand the fundamental physics of 2D materials. This method has remained almost unchanged over the past several years except for some modifications to increase the area of the exfoliated flakes. Huang et al. have achieved an area more than 50 times by employing additional oxygen plasma cleaning and heat treatment to the conventional exfoliation process(Huang et al., 2015).

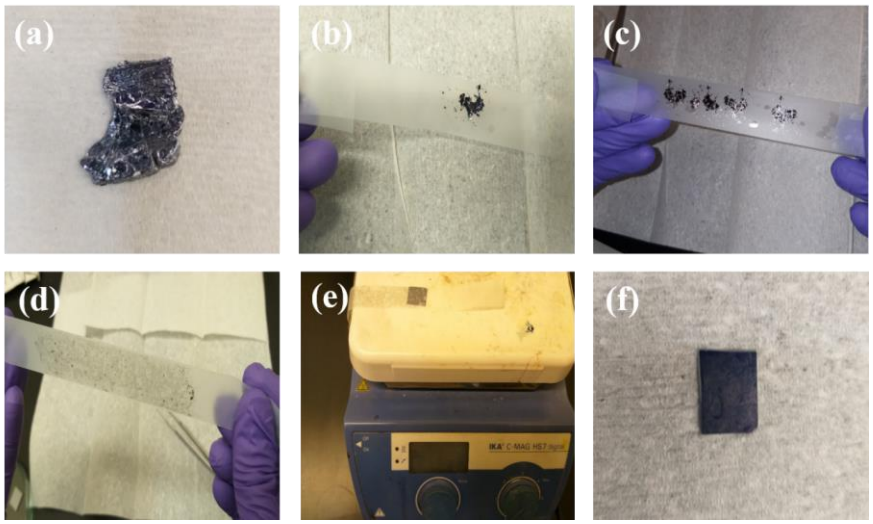

Figure 2.1: Illustration of the mechanical exfoliation process of MoS2. (a) Commercially available crystal of molybdenite (SPI Supplies). (b) Optical image of scotch tape after making contact with the crystal. (c) Repeated peeling off the scotch tape. (d) Further thinning down of MoS2 flakes after repeated peeling process. (e) Heating of the substrate in the air at 100 ˚C prior to removal of tape from the substrate. (f) Optical image of SiO2/Si after the MoS2 exfoliation process.

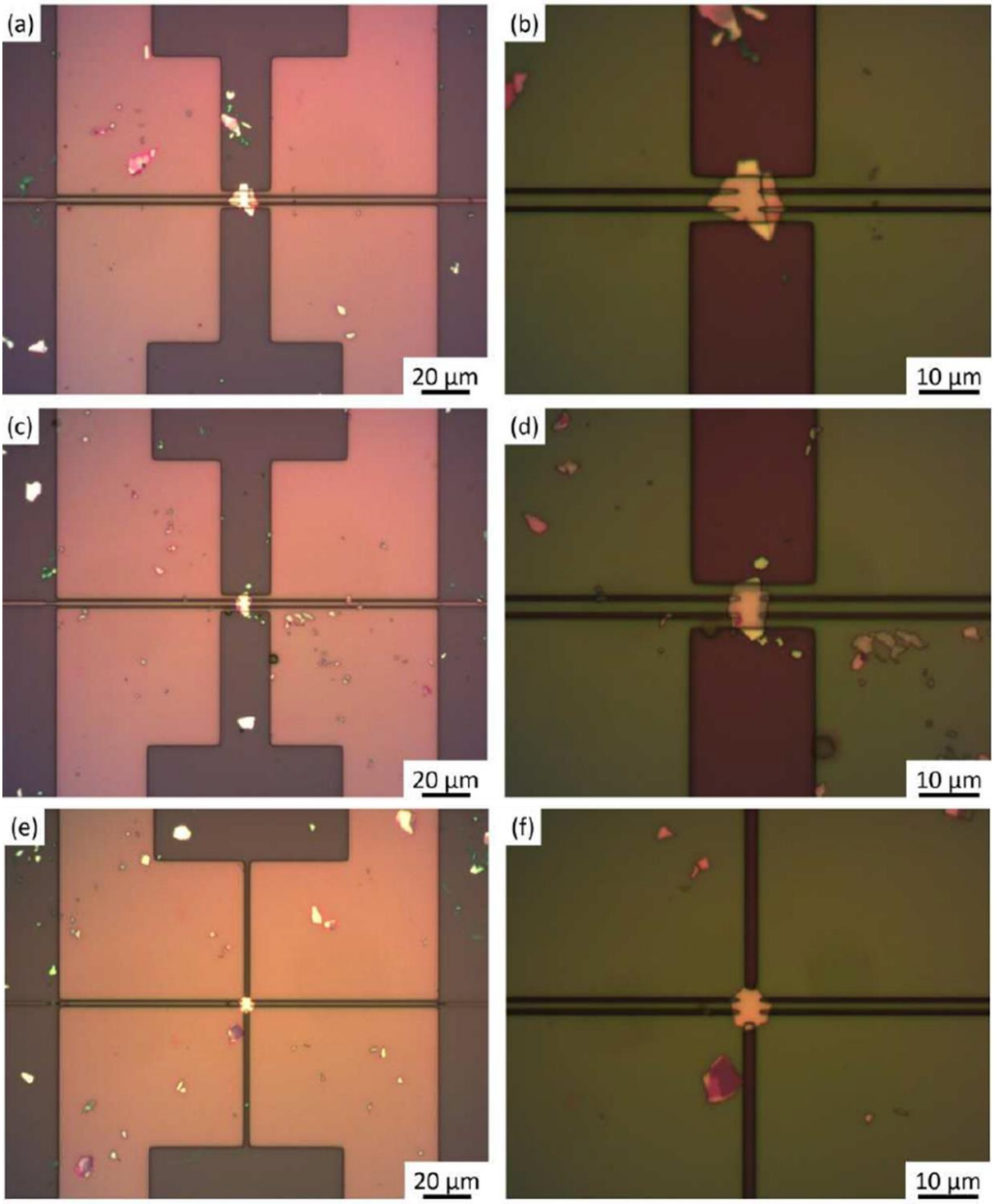

Figure 2.2: Optical microscope images of several contacted MoS2 flakes. All patterns were fabricated using the 0.6 µm resolution lens. (a), (b): Flake 1. (c), (d): Flake 2. (e), (f): Flake 3.

2.1.2 Chemical vapor deposition (CVD)

Although mechanical exfoliation provides flakes with very high crystallinity and superior electrical qualities. However, this method is not scalable as the typical flake size is

limited to few micrometers. Therefore, this method is only suitable for research applications and is not appropriate for commercial applications.

Over the past few years, CVD has been used as one of the primary techniques to grow large-area 2D materials over various substrates(Cai et al., 2018). In CVD, high-quality 2D materials are grown at a reasonable cost using different precursors. The morphology of the grown film can easily be changed according to a specific requirement by controlling the CVD growth parameters. The change in pressure and temperature changes the interface reactions, which lead to different structures. The schematic illustration of CVD process is shown in Figure 2.3.

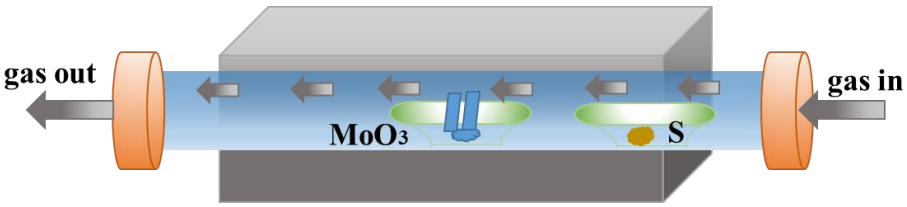

Figure 2.3: Schematic illustration of conventional chemical vapor deposition (CVD) technique for the growth of MoS2 film.

The experimental setup of our CVD system has been shown in Figure 2.4. Here, we have used MoO_3 and S as the precursors for the deposition of MoS_2 films. However, this CVD method provided a limited thickness control and resulted in non-uniform film deposition over a large area. In recent years, some modifications have occurred in conventional CVD to make it more efficient. One such modification is sulfurization of a pre-deposited metal layer, which we will discuss in the next section.

Figure 2.4: Optical image of chemical vapor deposition (CVD) system.

2.1.3 Sputtering coupled with sulfurization

For growing high quality, wafer-scale, and a uniform thin film of 2D material, modifications have to be made in the conventional CVD system. In this section, we will discuss one such modification, namely, pre-deposited sputtered metallic film coupled with sulfurization(Goel et al., 2018). In this technique, the thickness of the deposited MoS_2 film mainly depends on the pre-sputtered metallic film. Therefore, by controlling the thickness of the pre-deposited Mo film, we can scale the thickness of deposited MoS_2 film from few-layers to single atomic layers. By using this technique, highly homogenous and continuous films can be deposited over large areas of the substrates.

The working principle of magnetron sputtering techniques is shown in Figure 2.5. In the sputtering system, the target of the material which is to be coated on the substrate is fixed on a magnetron cathode. After fixing the target, the chamber is firstly evacuated to a rough vacuum and then to an ultrahigh vacuum by a rotatory pump and turbo pump, respectively. Pure Ar or Ar combined with other gases, is used to fill the chamber up to a certain pressure. A particular power is then applied to the magnetron, which creates an electric field between the sputtering target and substrate. Under the electric field, the electrons start accelerating and collided with Ar creating ions. A certain portion of these ions hits the target and sputter off the target material. The ejected target atoms then traveled towards the substrate under a high vacuum condition and formed a uniform film over the substrate.

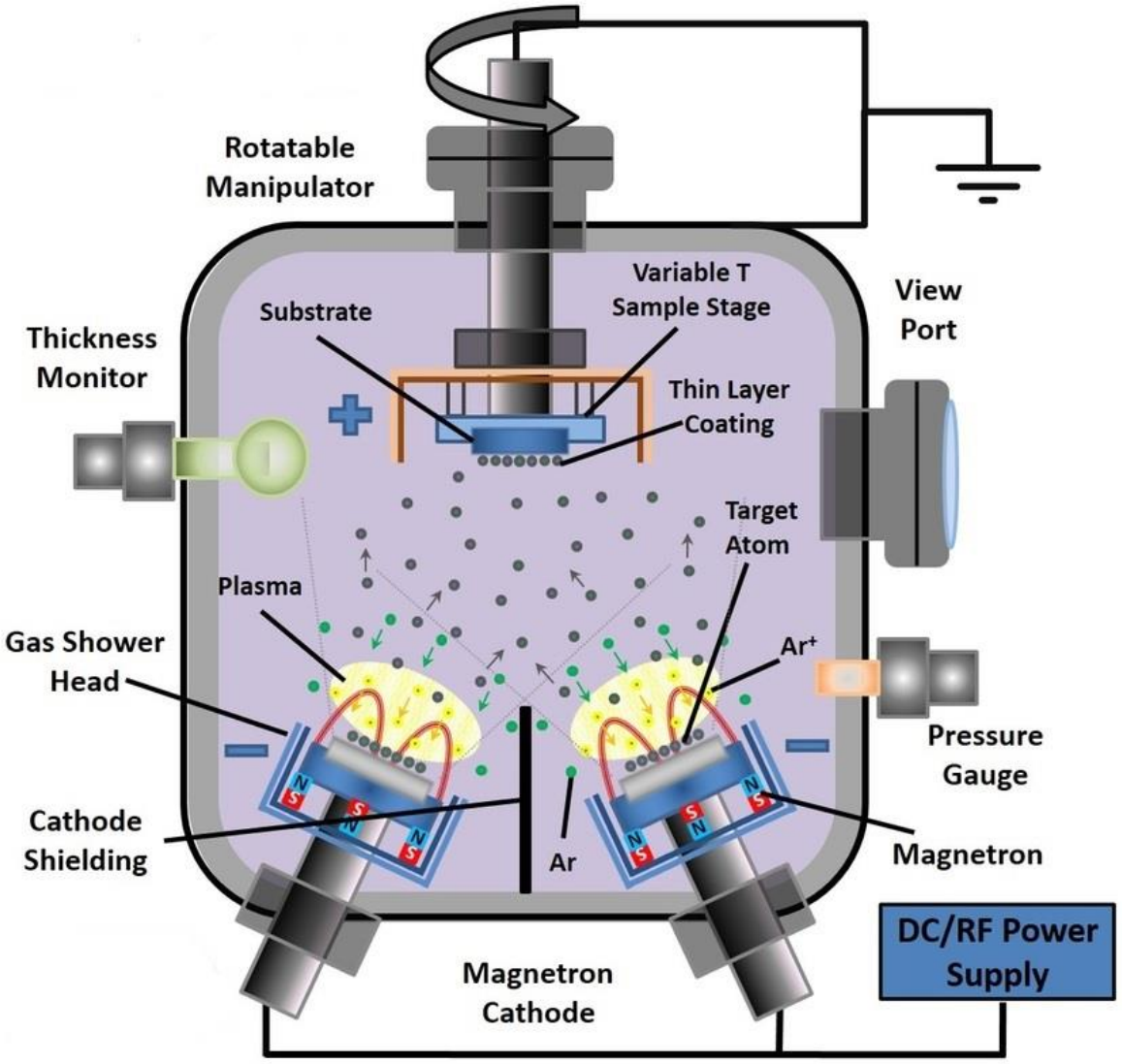

Figure 2.5: Working principle of magnetron sputtering technique. (Source: https://www.adnano-tek.com/magnetron-sputtering-deposition-msd.html)

This is a two-step method. In the first step, a thin layer of Mo is deposited using DC sputtering technique. The experimental setup of sputtering system is displayed in Figure 2.6 and deposition parameters for the deposition of Mo thin film are shown in Table 2.1.

Table 2.1: Deposition parameters of the pre-sputtered metallic film (Mo) on various substrates.

Substrates	SiO_2, Si, GaN
Sputtering target	Molybdenum (99.99 purity)
Base pressure	2×10^{-6} mbar
Working Pressure	6.5×10^{-3} mbar
DC power	40 W
Substrate temperature	600 °C
Ar gas flow	40 sccm
Deposition rate	6 nm/min
Target to substrate distance	5 cm

In the second step, the deposited metallic film is sulfurized in a sulfur-rich environment. The schematic illustration of both the steps are shown in Figure 2.7. The SEM images and their corresponding EDX spectra of some of the grown MoS_2 samples are shown in Figure 2.8. The EDX spectra confirms presence of O, Mo, and S as the main elements.

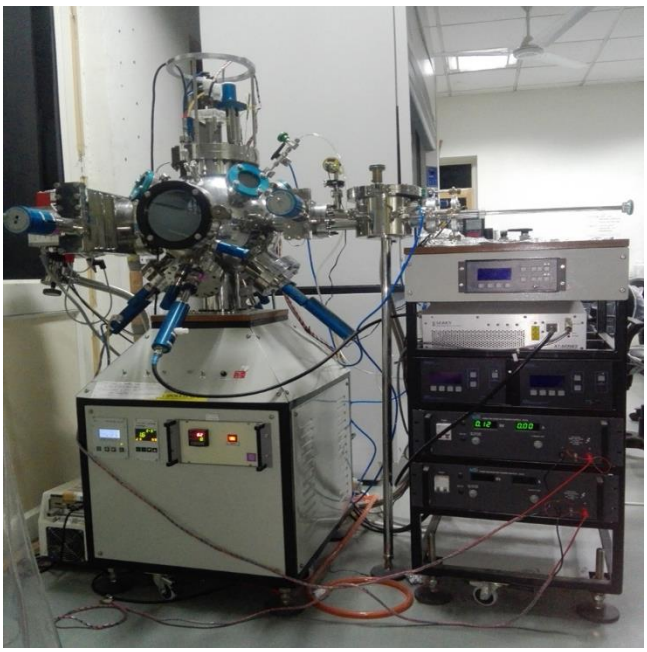

Figure 2.6: Experimental setup of magnetron sputtering system.

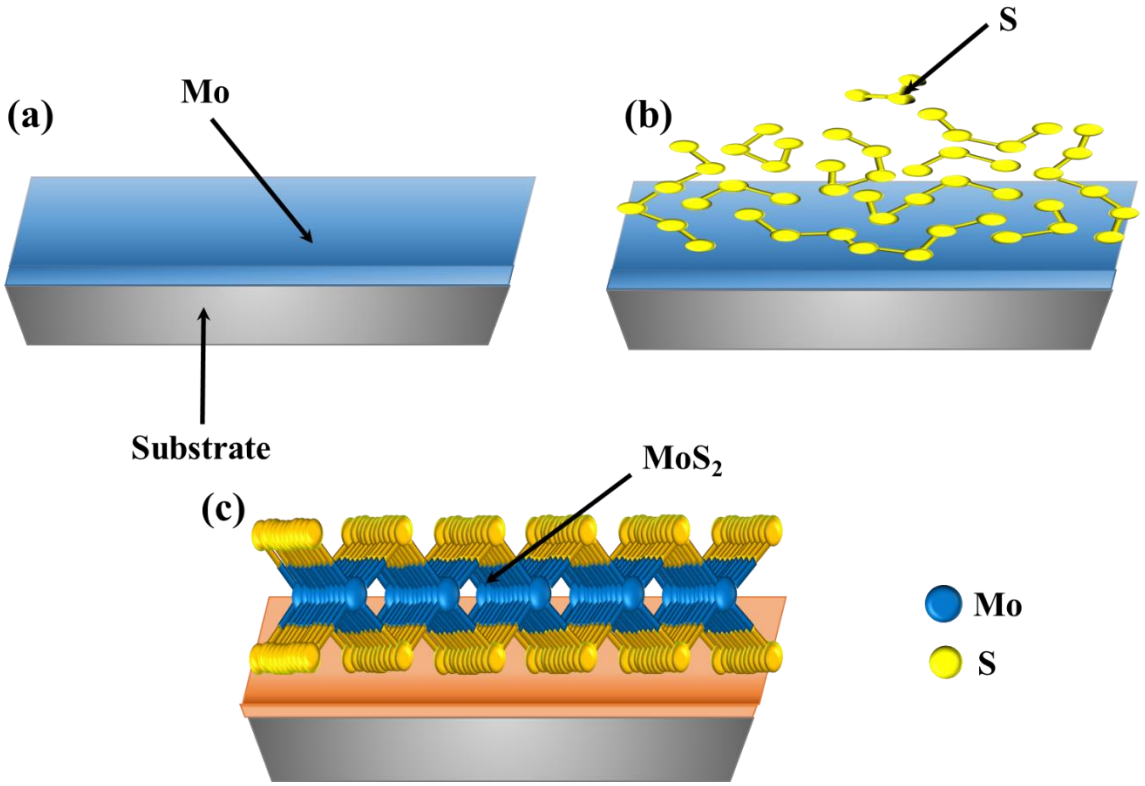

Figure 2.7: Schematic illustrations of fabrication process of growth process of MoS_2 film by Sputtering coupled with sulfurization technique. (a) The pre-deposited Mo film through DC sputtering technique. (b) Sulfurization of pre-deposited Mo film in sulfur-rich environment. (c) MoS_2 film grown on the substrate.

2.2 CHARACTERIZATION TECHNIQUE

2.2.1 Scanning electron microscopy (SEM)

In the field of material characterization, SEM is one of the most widely used techniques to study the morphology of the surface of the deposited films. Using this technique, the shape, size, and topography of the sample surface can easily be obtained through scanning the surface using an electron beam. With increasing miniaturization of the devices, it is not possible to characterize every structure with optical microscopy. For example, nanowires, nanofibers, nanoflowers, nanobelts, etc. are characterized by electron microscopy techniques. Optical microscopy cannot provide a very high-quality image in nm due to their poor resolution, while SEM gives a very high-quality image due to the smaller wavelength of electrons resulting in much higher resolution. The instrumental setup of SEM is shown in Figure 2.9.

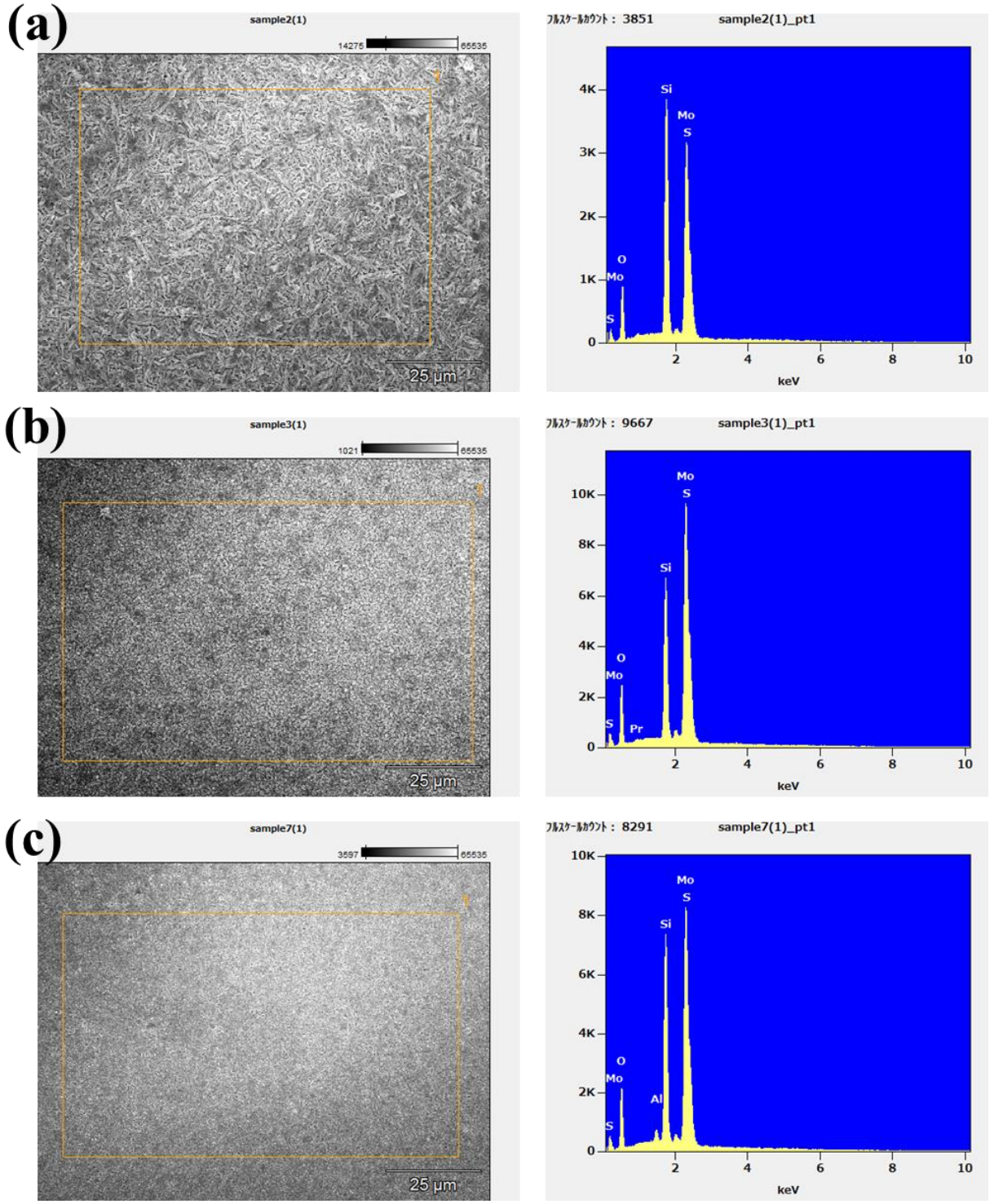

Figure 2.8: SEM images and corresponding EDX spectra of grown MoS2 through sputtering coupled with sulfurization technique. (a) Sample 2, (b) sample 3, and (c) sample 7.

The high energy electron and sample surface interaction provide information about the morphology and chemical composition of the deposited film. The detailed scanning process is illustrated in Figure 2.10. An electron beam is generated using either tungsten cathode or lanthanum hexaboride (LaB_6) cathodes. The emitted electron beam is focused by passing it through condenser lenses. After that, the focused beam is passed through deflection coils and the final lens aperture and then interacts with the sample surface. The incident electrons leave their energy through various elastic and inelastic scatterings, which in turn generate secondary electrons. The secondary electrons are detected by specific detectors producing the topographic

image of the sample surface. Using this technique, generally, a 2D image is captured over a specific area on the sample surface.

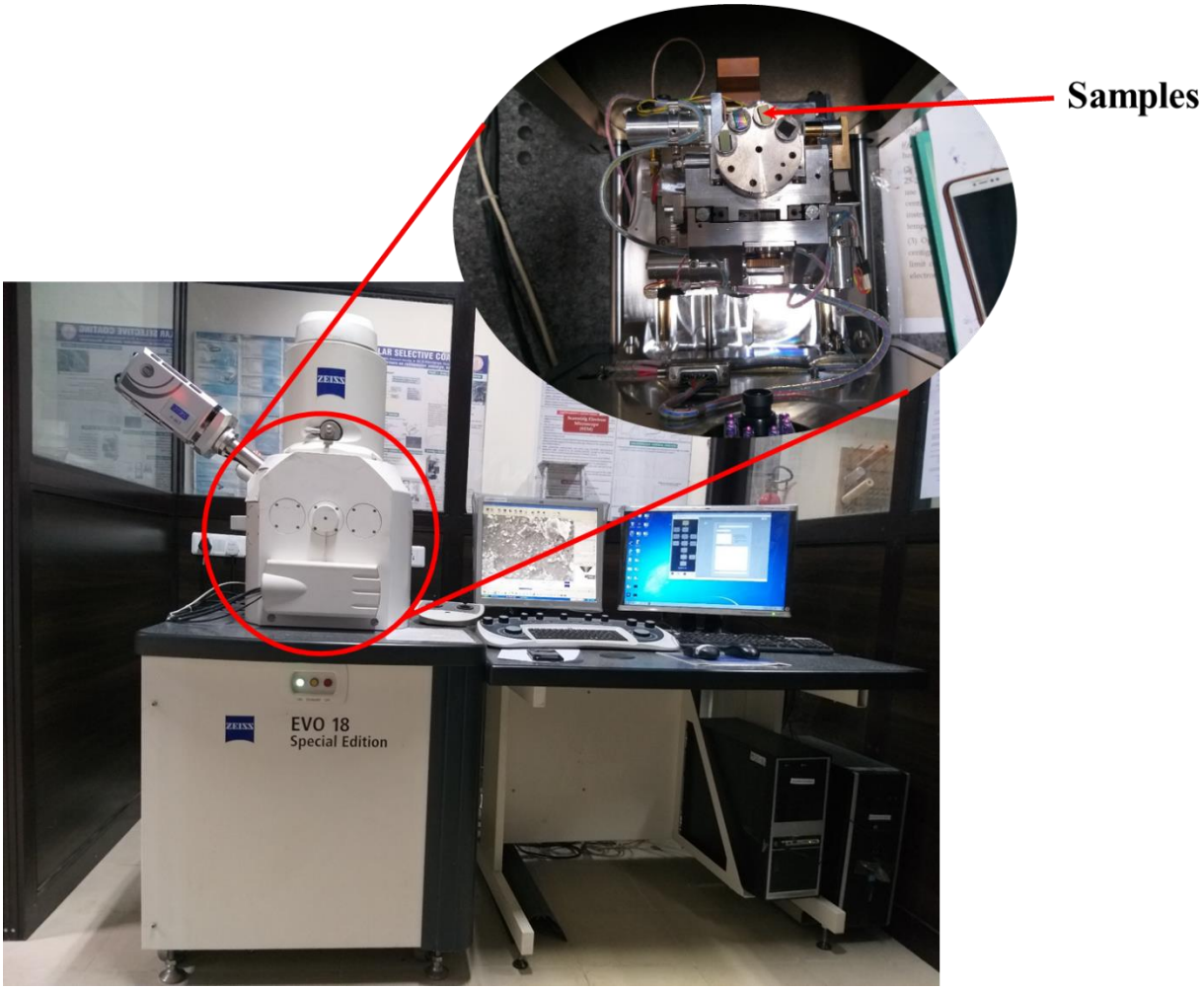

Figure 2.9: Experimental setup of scanning electron microscopy (SEM) system.

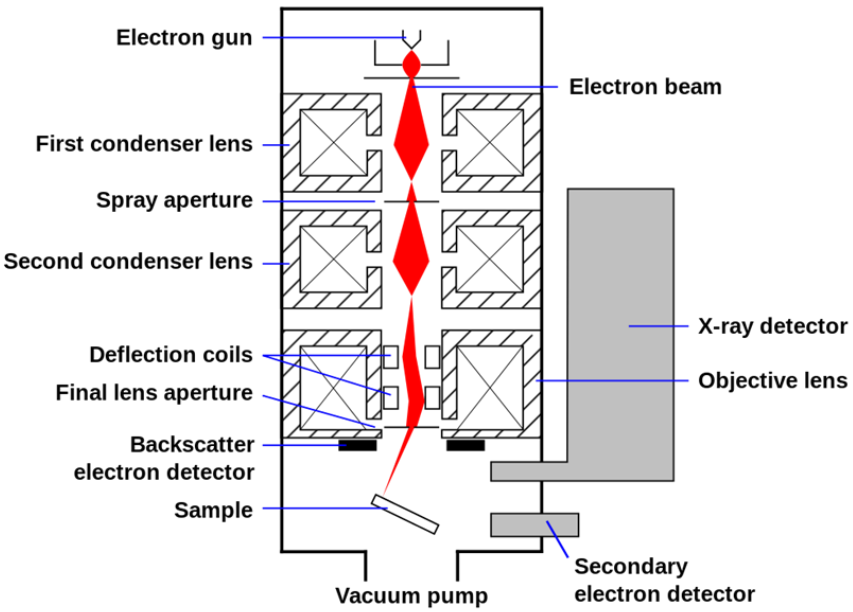

Figure 2.10: Working principle of SEM. (Source: https://en.wikipedia.org/wiki/Scanning_electron_microscope)

2.2.2 Atomic force microscopy (AFM)

AFM is one of the most widely used microscopy techniques to analyze the three-dimensional morphology of various substrates with atomic-scale resolution. Apart from the morphology, it also provides information about the height profile with a high value of precision level. The height profile of most of the deposited 2D materials through mechanical exfoliation is determined through the AFM technique, as this technique does not require any specific sample preparation. The principle of operation of AFM is shown in Figure 2.11. A tip attached to a cantilever is used for scanning the sample surface. As the tip scans the surface, the deflection of the cantilever and change in the direction of the reflected laser beam is recorded. An AFM image can easily be obtained by scanning the AFM tip over the area of interest. The different topography of the sample surface can be tracked by using photosensitive photodiode.

In the AFM technique, we can scan the tip while keeping the sample position stationary or by scanning the sample while keeping the tip stationary. In general, tip scanning is used over sample scanning because of its flexibility. This Technique plays a crucial role in characterizing 2D materials. The confirmation of isolation of graphene using mechanical exfoliation methods in 2004 was done using the AFM technique. The properties of 2D materials strongly depend on the number of layers. For instance, some 2D materials have direct bandgap in monolayer form and indirect bandgap in few-layer or bulk form. Therefore, it is essential to know the exact thickness of deposited material, which is possible through the AFM technique. Figure 2.12 shows the experimental setup of AFM system used in this thesis work.

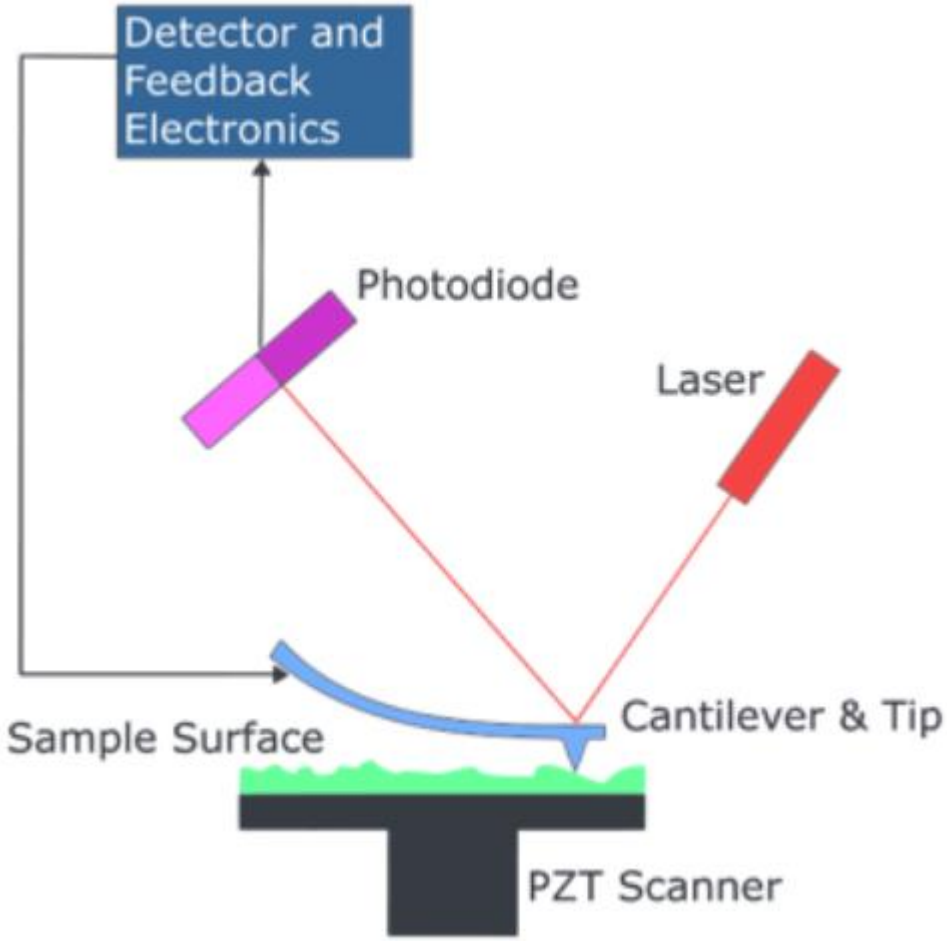

Figure 2.11: Working principle of AFM. (Source: http://physics.usask.ca/~chang/homepage/STMAFM/STMAFM.html)

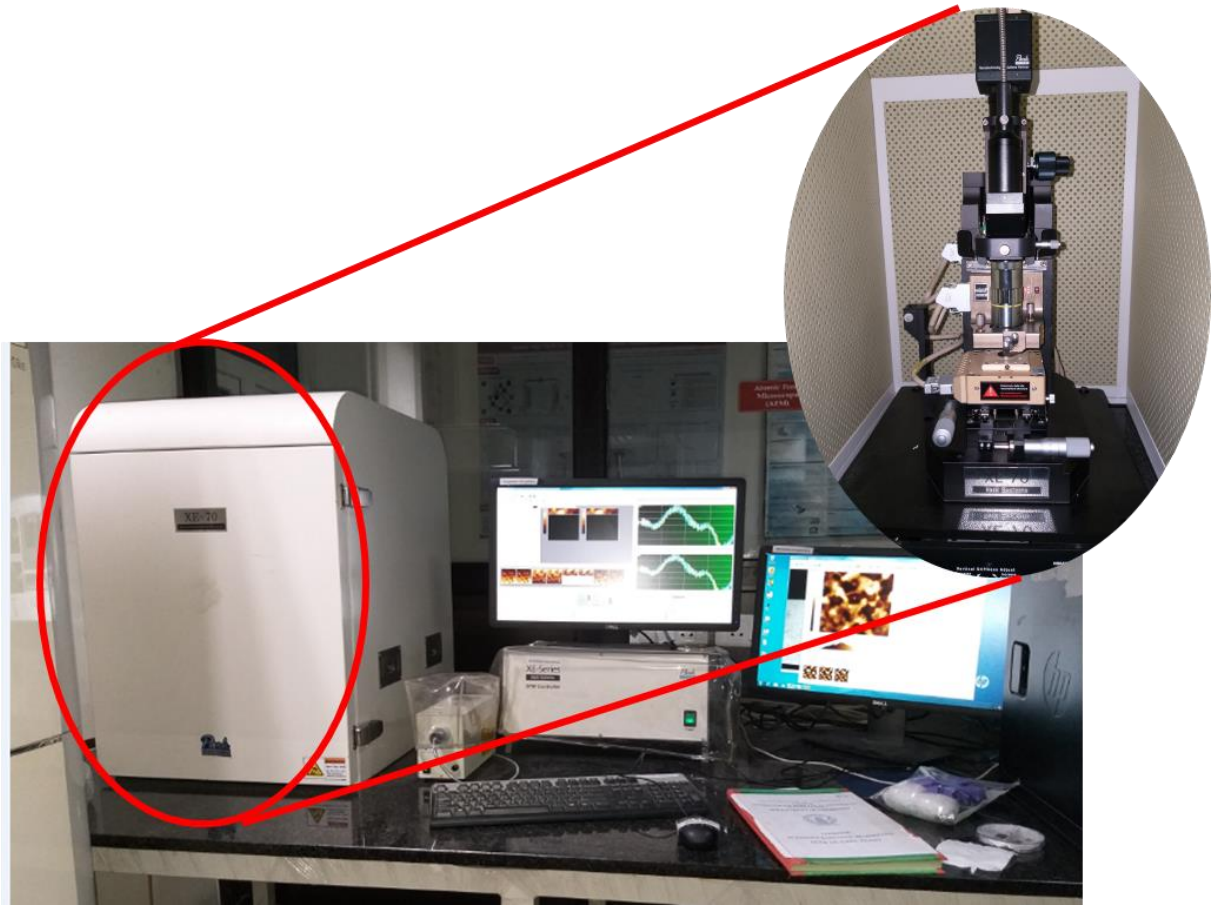

Figure 2.12: Instrument setup of atomic force microscopy (AFM) technique.

2.2.3 Raman Spectroscopy

In conventional bulk materials, the properties do not have any direct relation with their dimensions. However, the properties of 2D materials strongly dependent on the dimensions of the deposited materials. Raman Spectroscopy provides a robust and reliable approach for examining the layer thickness and changes in the material properties with thickness. The interfacial dynamics on the surface of TMDs and heterointerfaces can easily be understood using the Raman spectroscopy technique. The study of thickness scaling effect on the barrier-forming between TMDs and metallic contacts is essential for tailoring the potential barrier at the interface.

When light interacts with the sample, a part of it is reflected, the other part is absorbed, and the remaining part is scattered. In Raman spectroscopy, the scattering light is used to get information about different vibrational modes. The major portion of this scattered light is elastic, called Rayleigh scattering. Only a very small portion of this scattering is inelastic, which is referred to as Raman scattering, as shown in Figure 2.13. This Raman scattering consists of Strokes and anti-Strokes scattering. In anti-Strokes scattering, the molecules reach the higher state after gaining the energy from the photons, and their wavelength increases during the relaxation process. On the contrary, during Strokes, scattering wavelength of molecules decreases after the relaxation process.

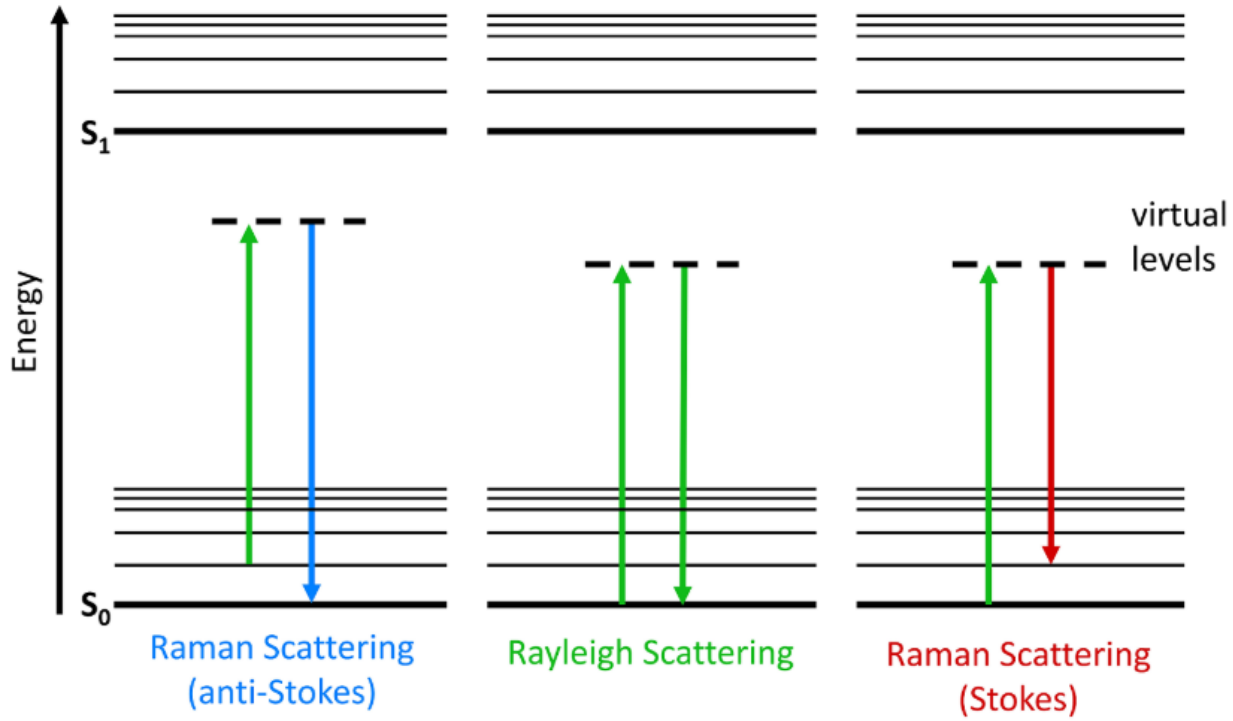

Figure 2.13: Occurrence of Rayleigh and Raman scattering (Stokes and Anti-Stokes). (Source: https://www.edinst.com/blog/what-is-raman-spectroscopy/)

Raman spectroscopy is a widely used non-destructive and convenient technique for the characterization of TMDs and other atomically thin 2D materials. The Raman modes in TMDs are highly thickness-dependent(Li et al., 2014). The frequency of Raman modes changes with change in thickness. Contact resistance, mobility, and bandgap change drastically with the change in the number of layers in TMDs due to quantum confinement. For instance, MoS2 is a direct bandgap material with a bandgap of 1.8 eV in its monolayer form, while it is an indirect bandgap material with a bandgap of 1.2 eV in its bulk form. The information regarding the lattice structure can also be extracted from the frequency of Raman phonon modes and the band structure by using the intensity due to resonance Raman scattering. Therefore, keeping an eye on the importance of Raman spectroscopy for the characterization of 2D materials, we have investigated different electronic and chemical properties of TMDs through Raman spectroscopy. Figure 2.14 displays the optical image of the Raman spectroscopy system.

Raman spectroscopy is essential to study the chemical and physical properties of 2D materials grown at the laboratory and mass-production scale. Most of the 2D based papers contain at least one Raman characterization to study electronic and vibrational properties of a material. Chen et al. have revealed quantum interference between different Raman pathways in graphene for understanding resonance Raman scattering in graphene(Chen et al., 2011). By using the Raman spectroscopy technique, Li et al. have demonstrated the evolution of the coupling between electronic transition and phonon when MoS2 is scaled down from three- to two-dimensional geometry(Li et al., 2012).

Figure 2.14: Instrument setup of Raman spectroscopy. (Courtesy: Material Research Centre, MNIT Jaipur)

2.2.4 Ultraviolet-visible spectroscopy

UV- Visible spectroscopy is one of the most popular characterization techniques to get an insight into the optical properties of a material. This technique measures the change in the absorption spectra of the sample with a change in illuminating wavelength. This technique uses ultraviolet to the visible range of the electromagnetic spectrum. Different phases of materials, including solid, liquid, or gaseous phases, can easily be analyzed using this method. Generally, the UV spectrum covers from 200 to 400 nm, while visible spectrum covers from 400 to 800 nm wavelength of the spectrum. The experimental setup of UV/Vis spectrophotometer is shown in Figure 2.15.

Figure 2.15: Experimental setup of UV/Vis spectrophotometer.

The different components used in UV-Vis spectroscopy are shown in Figure 2.16. It consists of light sources, diffraction grating, filters, mirrors, and a detector. Generally, two light sources are used in this technique to cover different spectral ranges. A deuterium lamp mainly covers the UV spectrum, while the tungsten lamp covers the visible portion of the spectrum. Depending on the requirement, a single lamp is used at a particular time. Photodiodes are used to detect the light. The light is passed through monochromators to ensure that only a particular wavelength arrives at the detector. The incident monochromatic light is divided into two equal parts before it interacted with the sample. One part is passed through the sample, while the other part works as a reference. By comparing the intensity of both the beams, the molecular structure, thickness, and other optical properties could easily be obtained.

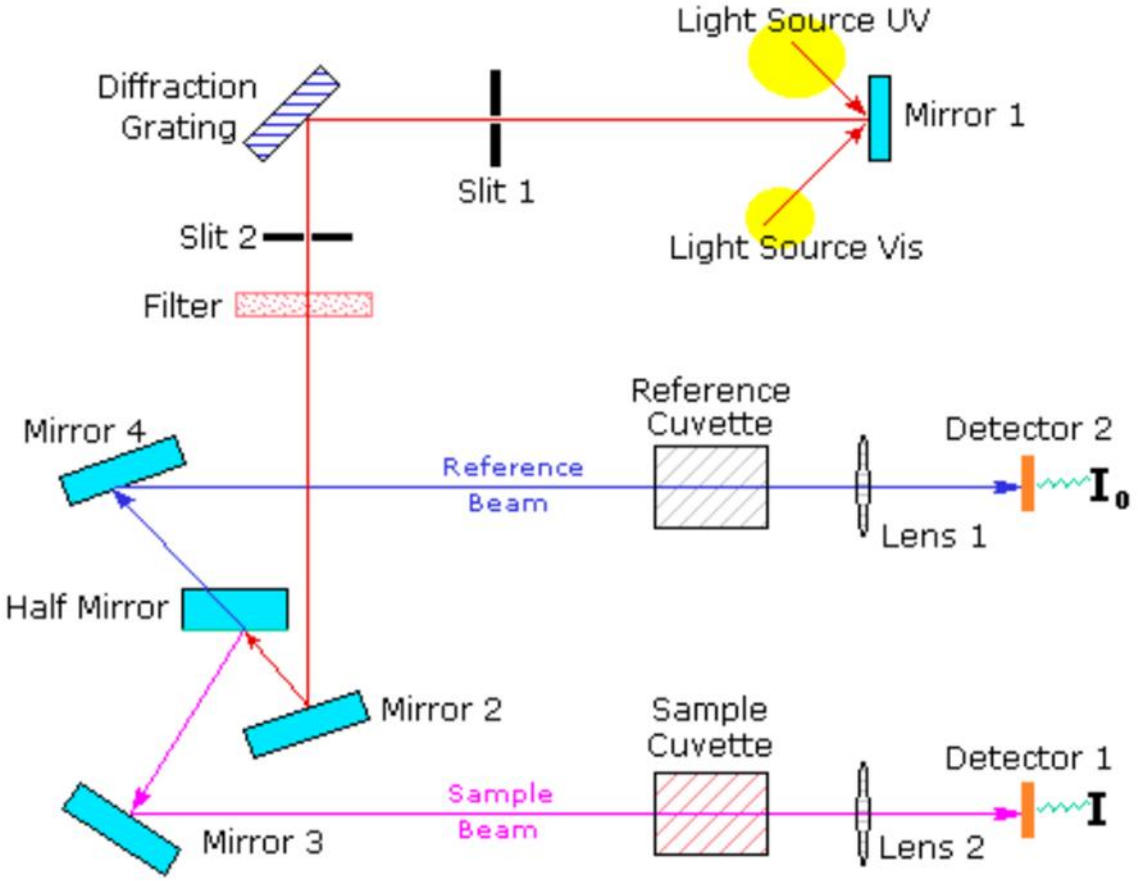

Figure 2.16: Principle of operation of UV/Vis spectrophotometer.

2.2.5 X-ray Powder Diffraction (XRD)

X-ray Powder Diffraction (XRD) is an analytical tool for studying the composition of solids, grain size, phase identification, and quality of crystalline materials. This technique also helps in determining the lattice parameters and atomic spacing of crystalline structures.

The principle of XRD depends on the constructive interference of monochromatic X-rays. A cathode-ray tube is used to produce the X-rays. The highly accelerated electrons are produced by heating the filament. Filtration of generated X-rays is necessary to convert them into monochromatic radiation. Finally, the monochromatic collimated to concentrate and allowed to fall on the sample. If the scattered X-rays follow Bragg's law, then constructive interference will take place, as shown in Figure 2.17(Sharma et al., 2012). Bragg's law is defined as:

$$2d\sin\theta = \nu\lambda \qquad (3.1)$$

Where d is the distance between crystallographic planes, θ is the incident angle and λ is the wavelength of the incident rays.

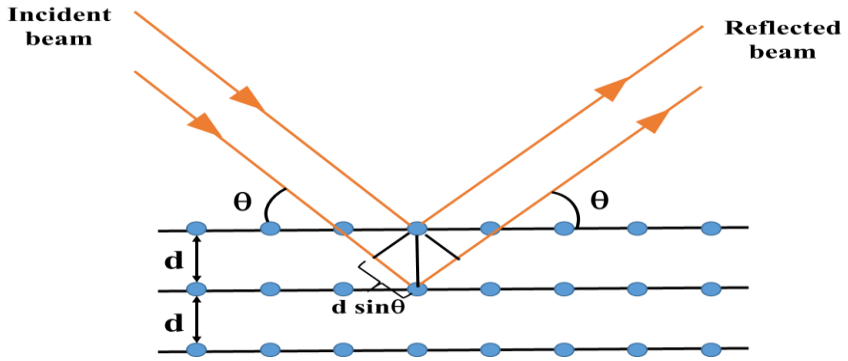

Figure 2.17: Schematic illustration of Bragg's x-ray diffraction process

The experimental setup of XRD used in our experiments is shown in Figure 2.18. The continuous movement of source and detectors through various angles results in different intensity diffracted X-rays, which is then recorded and processed.

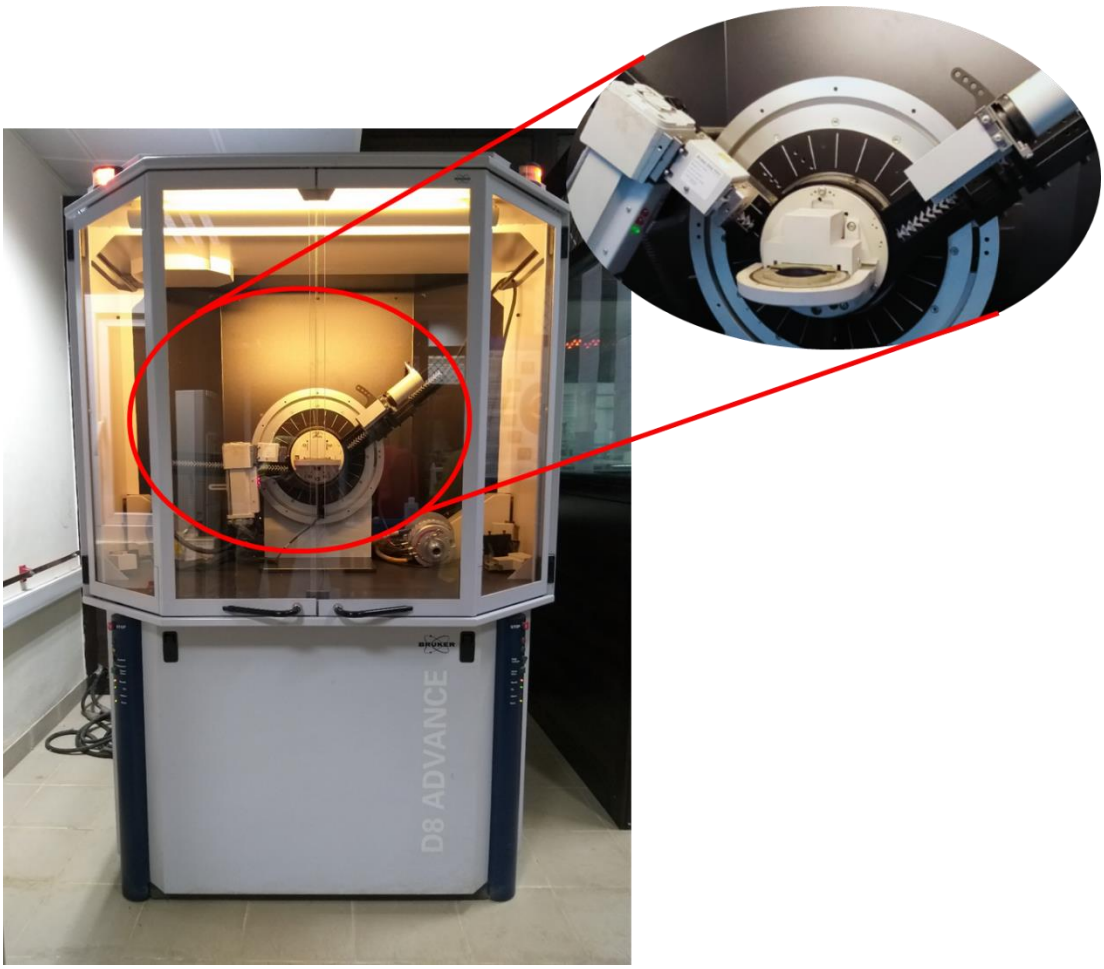

Figure 2.18: Optical image of the X-Ray diffraction (XRD) system.

2.2.6 X-ray photoelectron spectroscopy (XPS)

XPS is a highly sensitive spectroscopic process to identify the chemical state, chemical formula, and elemental composition within a solid material. We can also determine the crystal phase of the grown material by using this technique. XPS primarily worked on the principle of the

"photoelectric effect" as shown in Figure 2.19. X-rays are generated using either an Mg Kα or Al Kα source with photon energies of 1253.6 and 1486.6 eV, respectively. This technique requires an ultra-high vacuum (> 10^{-9} mbar) to confirm that the photogenerated electrons will not get scattered and have a large value of the mean free path. However, this technique gives the information typically from the top 10 nm of the studied sample.

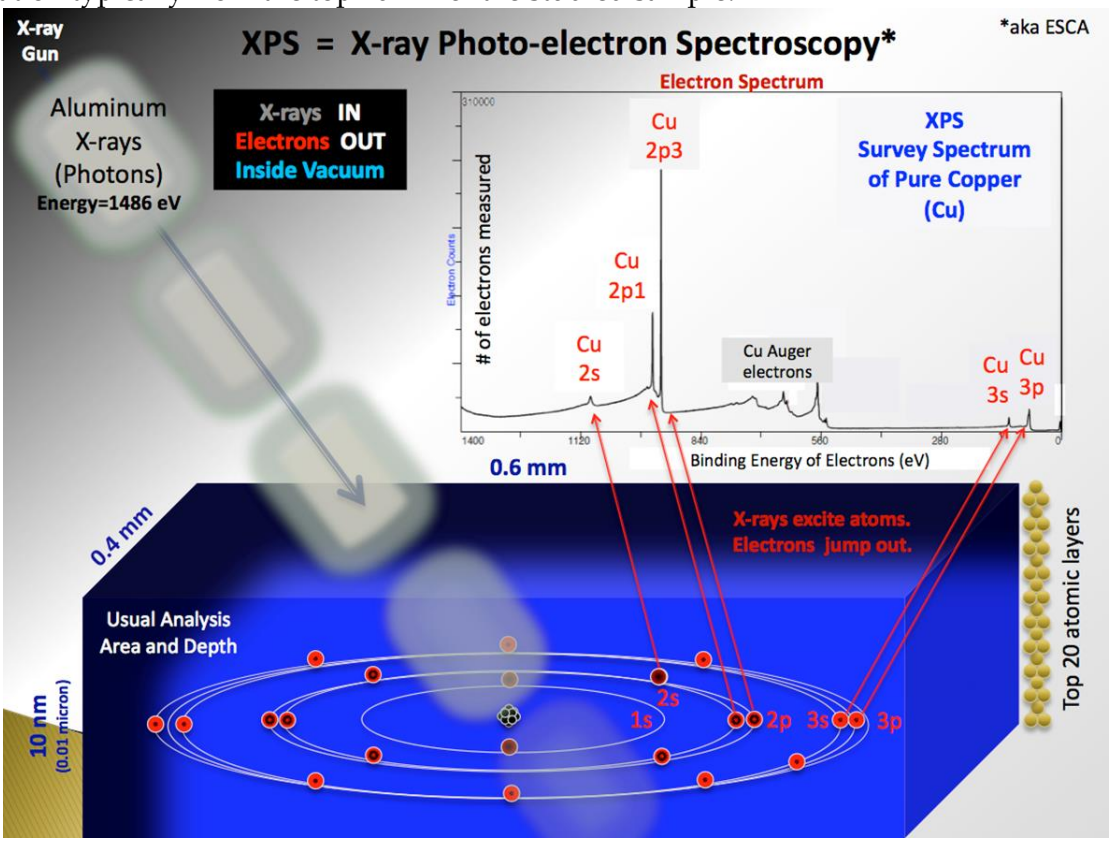

Figure 2.19: Schematic representation of working principle of the XPS technique. (Source: https://en.wikipedia.org/wiki/X-ray_photoelectron_spectroscopy)

Figure 2.20 shows the experimental setup of the XPS technique used in this thesis work. The sample is irradiated with the generated X-rays, which results in the ejection of electrons from the atoms of the sample due to the photoelectric effect, as illustrated in Figure 2.21. Depending upon a particular source, the energy of generated X-rays is known. Therefore, by measuring the kinetic energy of the ejected electrons, we can easily calculate the binding energy of the ejected electron by the following relation:

$$E_\beta = h\nu - E_{KE} - \phi \qquad (3.2)$$

Where E_b is the binding energy, $h\nu$ is energy of generated X-rays, E_{KE} is the kinetic energy of ejected electrons, and ϕ is work function.

Figure 2.20: Photograph of the X-ray photoelectron spectroscopy system, which is used for this thesis work. (Courtesy: Thin Film Devices & Metrology Section, CSIR-NPL New Delhi)

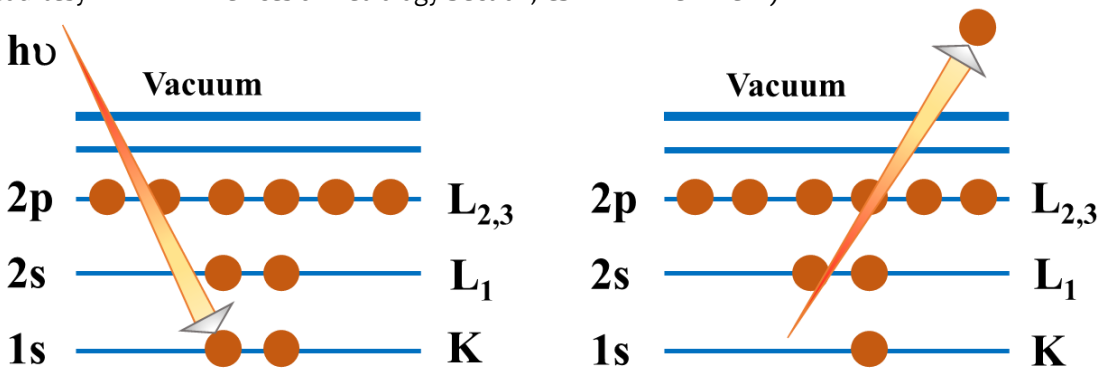

Figure 2.21: Schematic representation of the core electrons ejection process during XPS measurement.

2.2.7 Ultraviolet photoelectron spectroscopy (UPS)

UPS also works on the principle of the photoelectric effect, the same as that of the XPS technique. The key difference between XPS and UPS techniques is the source of irradiation. In UPS, a gas discharge lamp generally filled with helium is used to emit photons. The energy of the ejected photons by the discharge is either 21.2 eV using He I or 40.8 eV using He II source. Due to the large difference between irradiation energies in XPS and UPS techniques, there is a significant change in the penetration depth. The typical penetration depth in the case of UPS is ~5 nm, while in the case of XPS, the depth is ~10 nm. Therefore, UPS is more surface sensitive as compared to its XPS counterpart. The higher value of sensitivity results in a higher resolution (0.01 eV) of UPS technique. Moreover, the lower irradiation energy of ejected photons allows only valance band spectral acquisition, as shown in Figure 2.22. By using UPS, we can calculate the electron affinity, work function, and conduction band offsets of a particular material and their heterostructures(Tangi et al., 2017). In the present thesis work, we will demonstrate how to calculate the electron affinities and conduction band offsets using UPS techniques.

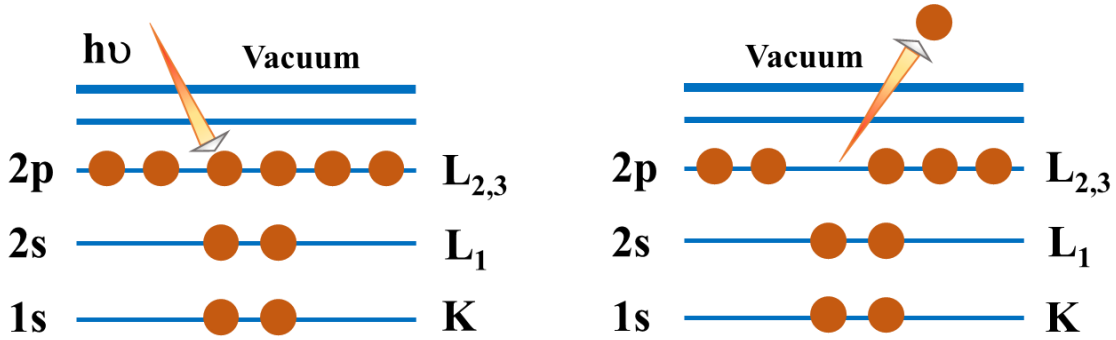

Figure 2.22: Schematic representation of valance electrons ejection process during XPS measurement.

2.3 CONTACTS PADS FORMATION

2.3.1 Thermal evaporator

Thermal evaporation is one of the most widely used physical vapor deposition techniques. A very high vacuum environment is a prerequisite for the thermal evaporation process. The high value of vacuum is required to increase the mean free path of vapor molecules larger than the separation between evaporation material and substrate. The high vacuum is also required to grow a high-quality film of evaporating material as the presence of oxygen or moisture can contaminate the deposited film. This technique has the advantage of a high deposition rate and exact real-time thickness control of deposited material. The experimental setup of the thermal evaporator is displayed in Figure 2.23.

Figure 2.23: Photograph of thermal evaporation system.

In the process, a material, which is going to be deposited on the substrate, is placed in a resistive boat and heated up to the evaporation point of the material. At evaporation point, surface atoms leave the surface and move towards the substrate, which is positioned on top of evaporating material. This high value of temperature is reached by applying a high value of

current across the resistive boat. A current of the order of hundreds of amperes is applied across the boat to heat it to a very high temperature. Therefore, these boats are made up of such a material that can sustain a very high value of temperature. The resistive boat is generally made up of tungsten or molybdenum. A crystal monitor is generally attached to the chamber to monitor the exact thickness of the deposited film. The samples which are to be coated are held by a substrate holder facing downward toward the crucible. The principle of operation of the thermal evaporator is illustrated in Figure 2.24. Both metallic and non-metallic films can be deposited using this technique. Generally, the thickness of the deposited film is in the range of nm. A layered structure using multiple materials is also possible by this process.

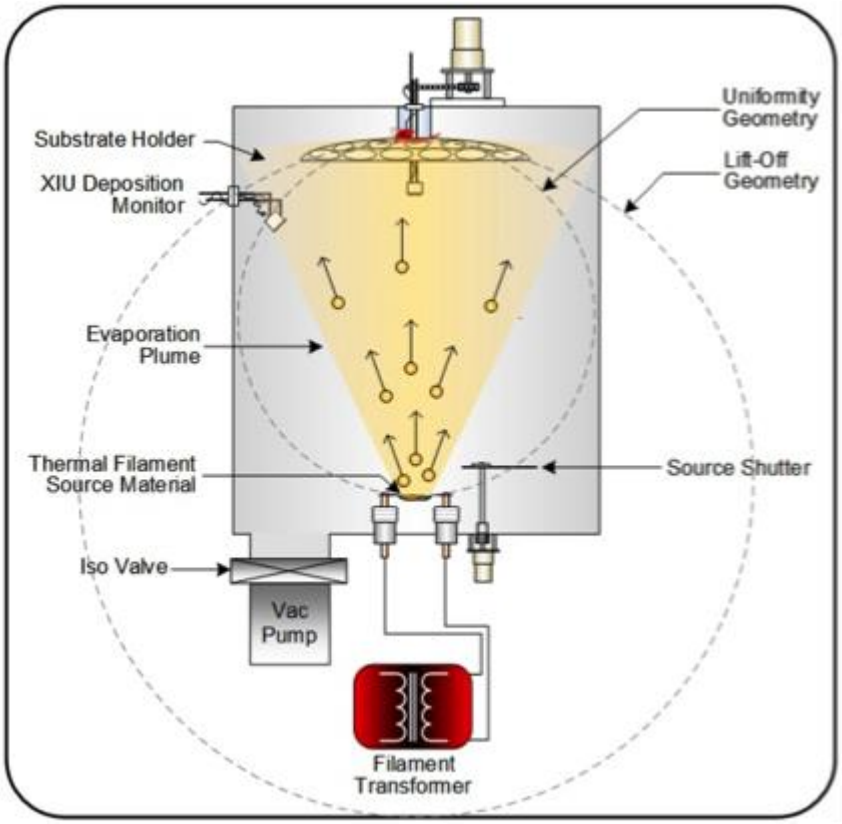

Figure 2.24: Working principle of thermal evaporation system. (Source: http://www.semicore.com/thin-film-deposition-thermal-evaporation)

2.3.2 Photolithography

Optical lithography is the process of printing a specific pattern on the substrate. In our lab, we have transferred different geometric patterns using a photomask. After cleaning the substrate, it is covered with photoresist using spin-coating techniques. The thickness of the photoresist depends on several factors, such as the speed of spin coater and the evaporation rate of solvents. After that, the substrate is prebaked for nearly 60 seconds. Then the prebaked substrate is exposed to UV irradiation using a photomask. Depending on the type of photoresist, the exposed or unexposed part is removed using a developer solution. Before developing a final pattern, a post bake process followed by a hard-baked process is used at optimized temperature and time duration. After further processing of substrates such as removal of deposition through wet chemical etching or ion implantation, the remaining photoresist is removed from the substrate using resist stripper. A pictorial representation of all the steps used during photolithography is shown in Figure 2.25. The resolution or the minimum feature size of the printed pattern primarily depends on the wavelength of the incident light and properties of the used lenses. The photograph of photolithography is shown in Figure 2.26.

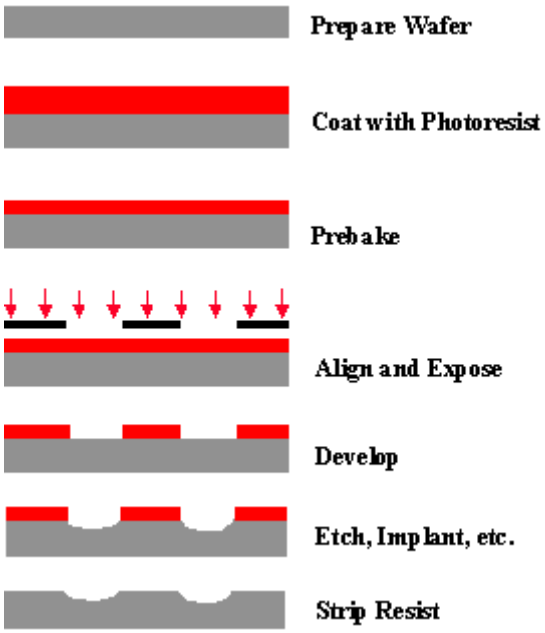

Figure 2.25: Sequential steps followed during the photolithography process.

Figure 2.26: Photograph of Mask Aligner: Optical Lithography.

2.4 MEASUREMENTS

2.4.1 Electrical measurements

The electrical characterization of various heterojunctions was done using two probes I-V characterization system. The probes were connected to Keithley 4200 parameter analyzer, as shown in Figure 2.27. By using it in different modes such as fixed voltage or voltage sweep, we can measure different electrical characteristics of the grown heterojunction. For example, once I-V characteristics are obtained, then we can easily calculate the barrier height, ideality factor, and contact resistance. The electrical characterization clearly illustrates the formation of the ohmic or Schottky barrier at the heterointerfaces.

The change in the photocurrent upon incidenting different wavelength light irradiation was also measured using this setup. In our experiments, we have used 365 nm (UV), 460 nm (blue), 520 nm (green), and 620 nm (red) light irradiation sources. The intensities of these light sources were calibrated using a commercial power meter from Holmark India.

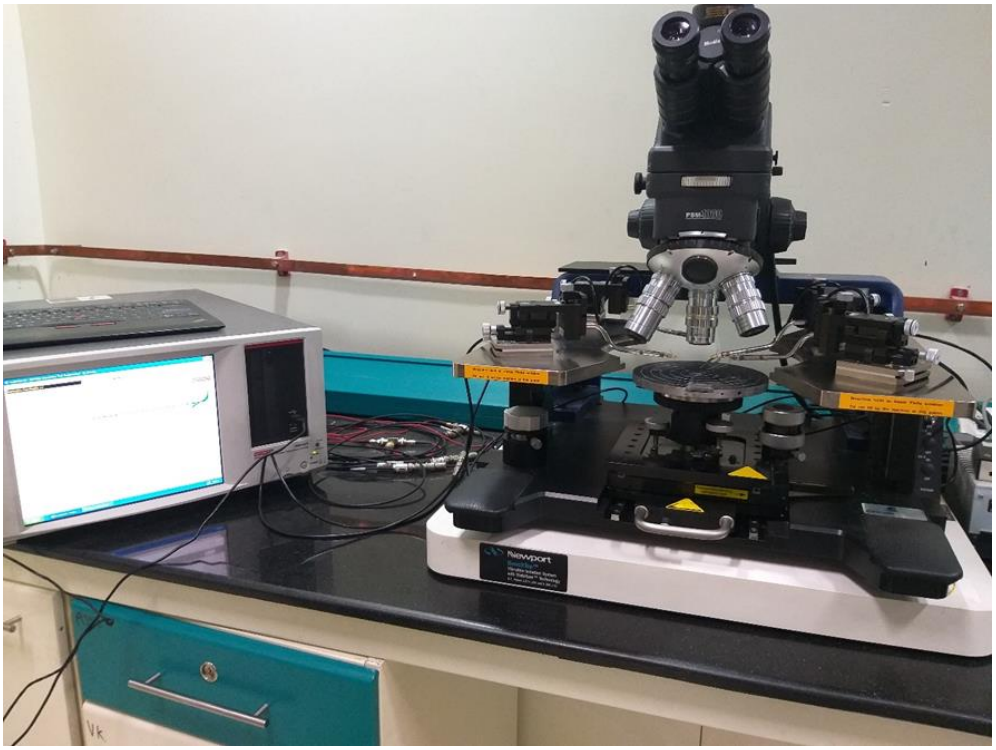

Figure 2.27: Instrument setup for electrical characterization.

2.4.2 Gas sensing measurements

The sensing performance of the device is evaluated in a customized closed gas sensing chamber. A rotary pump is attached to the stainless steel as a sensing chamber for evacuating gases from the chamber. Two probes are attached to a sample holder plated to make the electrical connection on metal electrodes for measuring device sensing behavior. The particular concentration of gas is then injected into the gas chamber through a mass flow controller. The gas is injected into the chamber through an inlet and moves out of the chamber through an outlet. The gas inlet can be connected to a mixer to modify the concentration of gases.

Here, we measure the relative change in the current or resistance upon exposure of various gases by using Keithley 4200-SCS source meter. The most commonly used gases are H2, CH4, NO2, NH3, CO2, and H2S. These gases are diluted to the desired concentration by mixing them with pure Ar in an appropriate proportion. The temperature of the sample can be

controlled from room temperature to 180 ˚C using external cartridge heaters through a PID temperature controller. The temperature of the device is kept constant during the experiment, which can be measured by an attached thermocouple. The customized gas sensing setup used in our lab is shown in Figure 2.28.

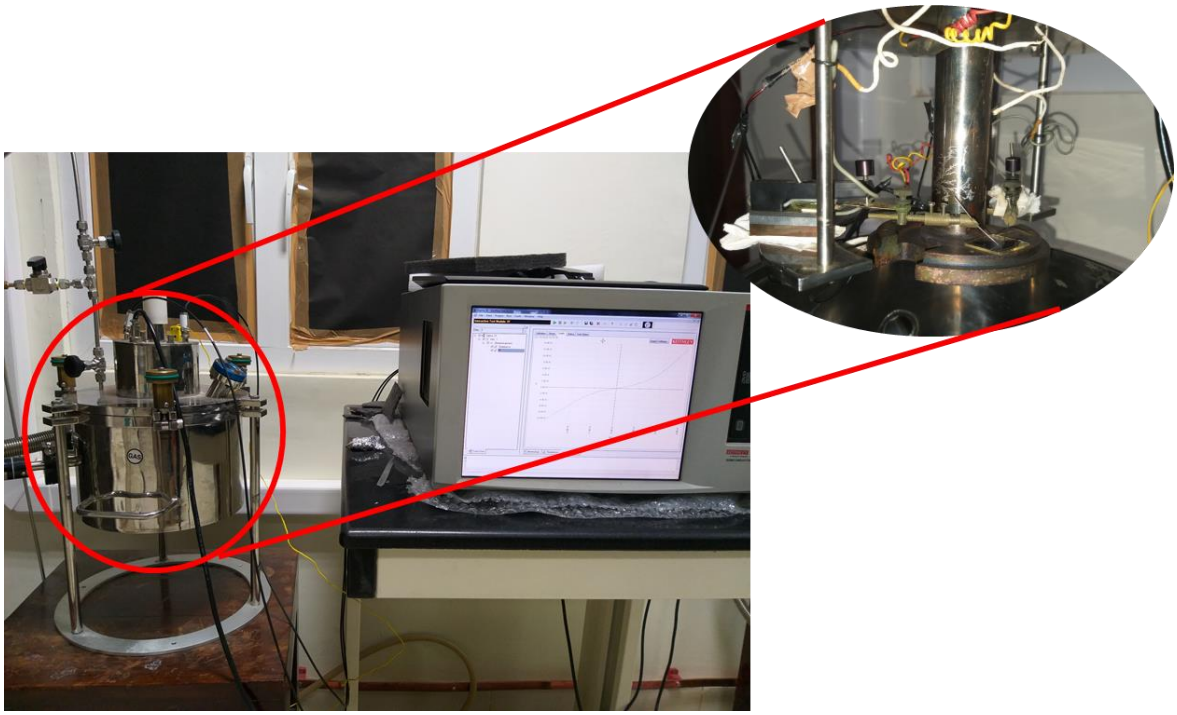

Figure 2.28: Experimental setup of customized gas sensing setup used in this thesis work.

…